

Expedited Optimization of Passive Microwave Devices Using Gradient Search and Principal Directions

Slawomir Koziel^{1,2}[0000-0002-9063-2647], Anna Pietrenko-Dabrowska²[0000-0003-2319-6782],
and Leifur Leifsson³[0000-0001-5134-870X]

- ¹ Engineering Optimization & Modeling Center, Department of Engineering, Reykjavík University, Menntavegur 1, 102 Reykjavík, Iceland
koziel@ru.is
- ² Faculty of Electronics Telecommunications and Informatics, Gdansk University of Technology, Narutowicza 11/12, 80-233 Gdansk, Poland
anna.dabrowska@pg.edu.pl
- ³ School of Aeronautics and Astronautics, Purdue University, West Lafayette, IN 47907, USA
leifur@purdue.edu

Abstract. Over the recent years, utilization of numerical optimization techniques has become ubiquitous in the design of high-frequency systems, including microwave passive components. The primary reason is that the circuits become increasingly complex to meet ever growing performance demands concerning their electrical performance, additional functionalities, as well as miniaturization. Nonetheless, as reliable evaluation of microwave device characteristics requires full-wave electromagnetic (EM) analysis, optimization procedures tend to be computationally expensive, to the extent of being prohibitive when using conventional algorithms. Accelerating EM-driven optimization is therefore a matter of practical necessity. This paper proposes a novel approach to reduced-cost gradient-based parameter tuning of passive microwave circuits with numerical derivatives. Our technique is based on restricting the finite-differentiation (FD)-based sensitivity updates to a small set of principal directions, identified as having the most significant effect on the circuit responses over the frequency bands of interest. The principal directions are found in the form of an orthonormal basis, using an auxiliary optimization process repeated before each iteration of the optimization algorithm. Extensive verification experiments conducted using a compact branch-line coupler and a dual-band power divider demonstrate up to fifty percent speedup obtained over the reference algorithm (using full FD sensitivity updates), as well as a considerable improvement over several accelerated algorithms. The computational savings are obtained with negligible degradation of the design quality.

Keywords: Microwave design, simulation-driven optimization, principal directions, gradient-based search, sparse sensitivity updates.

1 Introduction

Design of modern microwave components is a challenging endeavor. On the one hand, performance demands imposed on high-frequency systems become increasingly stringent, especially those associated with the emerging application areas (internet of things, IoT [1], wearable and implantable devices [2], 5G wireless communications). On the other hand, there is a growing trend to make the circuits more versatile (reconfigurability [3], multi-band operation [4], unconventional phase characteristics [5]). Another issue is miniaturization, which has become imperative in many cases due to the limitations on the physical space assigned for the passive circuitry [6], [7]. All these factors contribute to the increasing complexity of microwave components, which are described by many parameters, whereas their accurate evaluation requires costly full-wave electromagnetic (EM) analysis. As simpler models (e.g., equivalent networks) are no longer adequate, EM-driven optimization has become a necessity for parameter tuning. Yet, it is a computationally expensive procedure [8], which may require dozens, hundreds (gradient-based optimization over high-dimensional spaces), or even thousands of circuit simulations (global optimization [9], uncertainty quantification [10]).

The literature offers a large number of techniques for accelerating simulation-driven optimization of high-frequency components. In the context of local search, these include the employment of adjoint sensitivities [11], mesh deformation for fast sensitivity evaluation [12], feature-based methods [13], as well as cognition-driven design [14]. Surrogate-based optimization (SBO) is another and rapidly growing class of methods, which may involve both physics-based [15], and data-driven (approximation) models [16]. The latter (kriging [17], radial basis functions [18], support vector regression, neural networks [19]) are popular in global [20] and multi-criterial optimization [21], as well as statistical design [22]. Physics-based methods (space mapping [23], response correction techniques [15], [24]) are typically used in local search [25]. Unfortunately, SBO is affected by a number of issues, e.g., related to availability and setup of low-fidelity representations (physics-based models), or curse of dimensionality (data-driven models). Therefore, successful application examples of surrogate-assisted frameworks, are often limited to components described by a few parameters [26], [27].

Among the various optimization tasks, it is local parameter tuning that is by far the most often undertaken procedure in the case of high-frequency components, including microwave devices. The reason is the availability of reasonably good initial designs that are found through theoretical analysis or EM-based parametric studies. Local optimization is typically realized using gradient-based methods. Their computational efficiency mainly depends on the cost of estimating the gradients of the system characteristics. If adjoint sensitivities [11] are not accessible, the gradients are estimated through finite differentiation (FD). Acceleration is possible by restricting FD to selected system parameters, which may be decided upon based on investigating design relocation [28], detecting sensitivity patterns [29], or selective employment of updating formulas [30]. The aforementioned methods typically lead to at least forty percent speedup (in some cases, up to sixty) over full-FD updating schemes, with usually minor quality degradation. Yet, the efficacy depends on appropriate setup of the control parameters, which may be problem-dependent [28]-[30]. Also, sparse sensitivity updates are still limited

to the coordinate system axes. Performing the updates along arbitrary directions seems to be potentially more advantageous.

In this paper, we propose a novel technique for accelerated gradient-based design optimization of passive microwave devices. Our methodology restricts the finite-differentiation (FD)-based sensitivity updates to a small set of so-called dominant directions that are associated with the most significant variability of the system responses over the frequency bands of interest. The dominant directions form an orthonormal basis updated before each iteration of the optimization algorithm, and obtained by solving an auxiliary optimization sub-problem. In practice, only a few directions are used for sensitivity updating, which results in considerable computational savings. For the two microwave circuits used as verification case studies, the cost reduction is as high as fifty percent over the reference algorithm involving full-FD updates, without compromising the design quality. At the same time, the proposed procedure is faster than several accelerated versions previously reported in the literature.

2 Microwave Design Optimization Using EM Models

Here, we recall the formulation of microwave design optimization task, as well as discuss the standard trust-region gradient-based algorithm, which is the foundation for the accelerated procedure introduced in Section 3, as well as one of the benchmark algorithms considered in Section 4.

2.1 Optimization Task Formulation

Optimization of microwave circuits often requires handling of several characteristics (reflection, transmission, phase, etc.), performance figures (operating frequency/bandwidth, power split ratio), as well as constraints. For the sake of simplicity, the design task is most often formulated to minimize a scalar objective function, which aggregates the goals and constraints in a problem-dependent manner. Here, the parameter tuning problem is defined as

$$\mathbf{x}^* = \arg \min_{\mathbf{x}} U(\mathbf{x}) \quad (1)$$

where U is the merit (objective) function quantifying the design quality, \mathbf{x} is a vector of adjustable parameters, and \mathbf{x}^* is the optimum design to be found. Some examples of design tasks, and the corresponding objective functions can be found in Table 1. Therein, the following notation is used for the circuit S -parameters: $S_{kl}(\mathbf{x}, f)$, where f is the frequency, whereas k and l denote respective circuit ports.

2.2 Gradient-Based Search with Numerical Derivatives

In this work, we are concerned with local, gradient-based optimization of microwave components. As mentioned earlier, the major contributor to the computational cost is the evaluation of the circuit response gradients, which, in the absence of faster methods (e.g., adjoint sensitivities [17]), is realized through finite differentiation.

Our reference algorithm is the trust-region (TR) procedure [31]. Therein, the optimum design \mathbf{x}^* is approximated using a sequence of designs $\mathbf{x}^{(i)}$, $i = 0, 1, \dots$, found by solving

$$\mathbf{x}^{(i+1)} = \arg \min_{\mathbf{x}; -d^{(i)} \leq \mathbf{x} - \mathbf{x}^{(i)} \leq d^{(i)}} U_L^{(i)}(\mathbf{x}) \quad (2)$$

Table 1. Examples of microwave design optimization tasks

Design problem	Objective function	Comments
Design of an impedance matching transformer for minimum in-band reflection	$U(\mathbf{x}) = \max \{f \in F : S_{11}(\mathbf{x}, f) \}$	$ S_{11}(\mathbf{x}, f) $ is the circuit reflection; F is the frequency range of interest
Design of a dual-band coupler for the operating frequencies f_1 and f_2 . The objectives are to ensure equal power split, and to minimize the circuit matching and isolation at f_1 and f_2	$U(\mathbf{x}) = \max \{ S_{11}(\mathbf{x}, f_1) , S_{11}(\mathbf{x}, f_2) , S_{41}(\mathbf{x}, f_1) , S_{41}(\mathbf{x}, f_2) \} + \beta [(S_{21}(\mathbf{x}, f_1) - S_{31}(\mathbf{x}, f_1))^2 + (S_{21}(\mathbf{x}, f_2) - S_{31}(\mathbf{x}, f_2))^2]$	Minimization of matching and isolation is the primary objective. The second term is a penalty function enforcing equal power split
Design of a compact coupler for size reduction. The objective is to minimize the circuit footprint area $A(\mathbf{x})$, while maintaining a sufficient -20 dB bandwidth for $ S_{11} $ and $ S_{41} $, and equal power split at the operating frequency f_0 . The bandwidth is defined as $[f_0 - B, f_0 + B]$	$U(\mathbf{x}) = A(\mathbf{x}) + \beta_1 [\max \{c(\mathbf{x}) + 20, 0\} / 20]^2 + \beta_2 [S_{21}(\mathbf{x}, f_0) - S_{31}(\mathbf{x}, f_0)]^2$ where $c(\mathbf{x}) = \max \{f \in [f_0 - B, f_0 + B] : \max \{ S_{11}(\mathbf{x}, f) , S_{41}(\mathbf{x}, f) \}$	Function c quantifies a possible violation of the -20 dB level within the bandwidth of interest. The third term is similar to the second term in the second example.
Design of a triple-band power divider to operate at the frequencies f_1, f_2 , and f_3 . The objectives include ensuring equal power split, minimization of the input matching $ S_{11} $, output matching $ S_{22} $ and $ S_{33} $, as well as minimization of isolation $ S_{23} $ (all at f_1, f_2 , and f_3)	$U(\mathbf{x}) = \max \{ \max_{k, j \in \{1, 2, 3\}} S_{kk}(\mathbf{x}, f_i) , \max_{i \in \{1, 2, 3\}} S_{23}(\mathbf{x}, f_i) \} + \beta \sum_{i=1}^3 (S_{21}(\mathbf{x}, f_i) - S_{31}(\mathbf{x}, f_i))^2$	The second term is a penalty function enforcing equal power split at all operating frequencies.

In (2), the function $U_L^{(i)}$ is defined just as the original objective function U ; however, the circuit characteristics $S_{kl}(\mathbf{x}, f)$ are approximated using the respective linear expansion models

$$S_{L,kl}^{(i)}(\mathbf{x}, f) = S_{kl}(\mathbf{x}^{(i)}, f) + \nabla_{kl}(\mathbf{x}^{(i)}, f) \cdot (\mathbf{x} - \mathbf{x}^{(i)}) \quad (3)$$

The gradients of S_{kl} at the design \mathbf{x} and frequency f are defined as

$$\nabla_{kl}(\mathbf{x}, f) = \left[\frac{\partial S_{kl}(\mathbf{x}, f)}{\partial x_1} \dots \frac{\partial S_{kl}(\mathbf{x}, f)}{\partial x_n} \right] \quad (4)$$

It should be noted that the solution to sub-problem (2) is found in the interval $[\mathbf{x}^{(i)} - \mathbf{d}^{(i)}, \mathbf{x}^{(i)} + \mathbf{d}^{(i)}]$, the size of which is adjusted using the TR rules [31]. The computational cost of (2) is at least $n + 1$ EM simulations due to evaluation of (4) using finite differentiation. If the iteration fails, i.e., if $U(\mathbf{x}^{(i+1)}) \geq U(\mathbf{x}^{(i)})$, it is repeated with reduced $\mathbf{d}^{(i)}$. As mentioned earlier, the above procedure will be a benchmark algorithm in Section 4. It is also a basis for the procedure proposed in this work, as elaborated on in Section 3.

3 Accelerated Optimization by Means of Principal Directions

This section describes the proposed approach to accelerated parameter tuning of passive microwave devices. It is based on the concept of principal directions introduced in Section 3.1, and sensitivity updates restricted to a small set thereof, as elaborated on in Section 3.2. The complete optimization algorithm is summarized in Section 3.3.

3.1 Principal Directions and Their Identification

The proposed approach is based on restricting the finite-differentiation (FD) updates of the system sensitivity matrix to a few principal directions, which are the most influential in terms of response variability. This translates into a reduced operating cost of the optimization process.

In order to find the principal directions, we need to first decide upon the response variability metric F_v . It is defined by considering the frequency range of interest F , determined according to the design problem at hand. F can be a discrete set of target operating frequencies, or a continuous frequency interval, if the circuit characteristics are of interest over a specified bandwidth. The variability of the S -parameter S_{kl} is defined as

$$F_{v,kl}(S_{kl}(\mathbf{x}_1), S_{kl}(\mathbf{x}_2)) = \sqrt{\int_F [|S_{kl}(\mathbf{x}_1, f)| - |S_{kl}(\mathbf{x}_2, f)|]^2 df} \quad (5)$$

Which, in the case of a discrete set of frequencies $f_j, j = 1, \dots, p$, becomes

$$F_{v,kl}(S_{kl}(\mathbf{x}_1), S_{kl}(\mathbf{x}_2)) = \sqrt{\sum_{j=1}^p [|S_{kl}(\mathbf{x}_1, f_j)| - |S_{kl}(\mathbf{x}_2, f_j)|]^2} \quad (6)$$

This can be generalized for multiple circuit responses $S_{kl}, \{k, l\} \in \{\{k_1, l_1\}, \dots, \{k_r, l_r\}\}$ (e.g., $k = 1, 2, 3, 4$, and $l = 1$, for a coupler structure), as the average of $F_{v,kl}$ for all characteristics involved

$$F_v(\mathbf{x}_1, \mathbf{x}_2) = \frac{1}{r} \sum_{j=1}^r F_{v,k_j l_j}(S_{k_j l_j}(\mathbf{x}_1), S_{k_j l_j}(\mathbf{x}_2)) \quad (7)$$

Our goal is to identify an orthonormal basis of vectors $\{\mathbf{v}^{(j)}\}_{j=1, \dots, n}$, ordered in a descending manner with respect to F_v . A small subset thereof will govern the sensitivity updates, cf. Section 3.2. Let $\mathbf{x}^{(i)}$ be the design found in the i th iteration of the optimization process, and let $S_{L,kl}^{(i)}(\mathbf{x}, f)$ be the linear model of S_{kl} at $\mathbf{x}^{(i)}$ (cf. (3)). We define

$$\mathbf{v}^{(1)} = \arg \max_{\mathbf{v}: \|\mathbf{v}\|=1} F_{L,v}(\mathbf{x}^{(i)} + \mathbf{v}, \mathbf{x}^{(i)}) \quad (8)$$

where

$$F_{L,v}(\mathbf{x}^{(i)} + \mathbf{v}, \mathbf{x}^{(i)}) = \frac{1}{r} \sum_{j=1}^r F_{v,k_j l_j}(S_{L,k_j l_j}^{(i)}(\mathbf{x}^{(i)} + \mathbf{v}), S_{k_j l_j}(\mathbf{x}^{(i)})) \quad (9)$$

According to (8), $\mathbf{v}^{(1)}$ maximizes the variability metric F_v in the vicinity of $\mathbf{x}^{(i)}$. The S -parameters at $\mathbf{x}^{(i)} + \mathbf{v}$ are estimated using the respective linear models in order to make the solution to (8) computationally feasible.

In order to find the remaining $n - 1$ directions, $\mathbf{v}^{(2)}, \mathbf{v}^{(3)}, \dots$, a process similar to (8) is executed with additional constraints imposed to ensure orthogonality of the vectors. Having $\mathbf{v}^{(k)}, k = 1, \dots, j$, $\mathbf{v}^{(j+1)}$ is identified as

$$\mathbf{v}^{(j+1)} = \arg \max_{\bar{\mathbf{v}}} F_{L,v}(\mathbf{x}^{(i)} + \bar{\mathbf{v}}, \mathbf{x}^{(i)}) \quad (10)$$

where $\bar{\mathbf{v}}$ has the form of

$$\bar{\mathbf{v}} = \frac{P^{(j)}(\mathbf{v})}{\|P^{(j)}(\mathbf{v})\|} \quad (11)$$

in which

$$P^{(j)}(\mathbf{v}) = \mathbf{v} - \sum_{k=1}^j \mathbf{v}^{(k)} [(\mathbf{v}^{(k)})^T \mathbf{v}] \quad (12)$$

It can be noted that (11) and (12) ensure that $\mathbf{v}^{(j+1)}$ has a unity length and it is orthogonal

to $\mathbf{v}^{(k)}$, $k = 1, \dots, j$.

Figure 1 provides a graphical illustration of the aforementioned concepts for a compact branch-line coupler. In the considered case, the majority of response changes occur along the first three directions, therefore, restricting the sensitivity updates to this subset seems reasonable.

3.2 Restricted Sensitivity Updates

The procedure for generating the principal directions ensures that $F_{L,v}(\mathbf{x}^{(i)} + \mathbf{v}^{(1)}, \mathbf{x}^{(i)}) > F_{L,v}(\mathbf{x}^{(i)} + \mathbf{v}^{(2)}, \mathbf{x}^{(i)}) > \dots > F_{L,v}(\mathbf{x}^{(i)} + \mathbf{v}^{(n)}, \mathbf{x}^{(i)})$, with only a few directions responsible for the majority of response changes in the vicinity of $\mathbf{x}^{(i)}$ (cf. Fig. 1). Consider the variability factors C_j determining the (relative) contribution of the first j directions to the overall response variation

$$C_j = \frac{\sqrt{\sum_{k=1}^j [F_{L,v}(\mathbf{x}^{(i)} + \mathbf{v}^{(k)}, \mathbf{x}^{(i)})]^2}}{\sqrt{\sum_{k=1}^n [F_{L,v}(\mathbf{x}^{(i)} + \mathbf{v}^{(k)}, \mathbf{x}^{(i)})]^2}} \quad (13)$$

The number j_{update} of directions utilized for the sensitivity updates can be computed based on the user-defined threshold C_{th} , typically set to 0.9 or higher. We have

$$j_{update} = \arg \min \{ j \in \{1, 2, \dots, n\} : C_j \geq C_{th} \} \quad (14)$$

Going back to Fig. 1, we would have $j_{update} = 2$ given $C_{th} = 0.95$. This means that the first two directions $\mathbf{v}^{(j)}$ contribute at least 95% of response variability as defined by (13). However, C_j are calculated using the linear models (3), which is an approximation. Therefore, in practice, it is recommended to introduce a lower bound on j_{update} at the level of about one third of the parameter space dimensionality, so that (14) is modified to $j_{update} = \max\{\arg \min\{j \in \{1, 2, \dots, n\} : C_j \geq C_{th}\}, \lceil n/3 \rceil\}$, where $\lceil \cdot \rceil$ stands for the ceiling function.

Having j_{update} , the S -parameter sensitivity is updated using EM simulations results at the design perturbed along the selected principal directions $\mathbf{v}^{(j)}$, $j = 1, \dots, j_{update}$. The perturbation data is incorporated using the Broyden formula [32], as illustrated in Fig. 2.

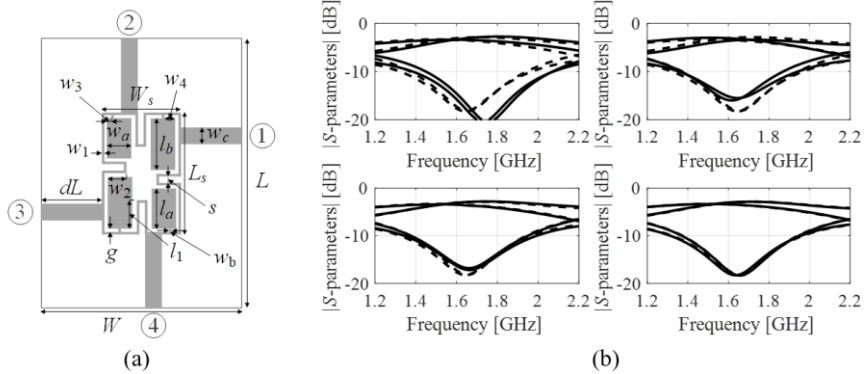


Fig. 1. Compact branch-line coupler and its S -parameter variability along the principal directions obtained using the procedure of Section 3.1: (a) circuit geometry, (b) EM-simulated S -parameters at the selected design $\mathbf{x}^{(i)}$ (---) and at $\mathbf{x}^{(i)} + h\mathbf{v}^{(j)}$ (—) for $j = 1, 2, 3$, and 4 (from top-left to bottom-right). Normalized response variability values are 1.00, 0.76, 0.19, and 0.07.

3.3 Optimization Algorithm

Figure 3 shows the flow diagram of the proposed optimization procedure with sparse sensitivity updates. The core optimization algorithm is the trust-region routine outlined in Section 2.2. The only control parameters are the threshold C_{th} (cf. Section 3.2), and the termination threshold ε that determines the resolution of the search process (set to $\varepsilon = 10^{-3}$ in the verification experiments of Section 4).

The sensitivities of the scattering parameters $S_{kl}(\mathbf{x}^{(i)})$, $k, l = 1, \dots, p$, are evaluated using FD in the first iteration of the algorithm, so that the principal directions can be identified with a sufficient accuracy. In further iterations, the gradients are updated using the EM-simulated circuit characteristics at the new design $\mathbf{x}^{(i+1)}$, and along the selected principal directions. The TR size vector $\mathbf{d}^{(i+1)}$ is updated based on the gain ratio r . The rules are as follows: if $r > 0.75$, then $\mathbf{d}^{(i+1)} = 2\mathbf{d}^{(i)}$; if $r < 0.25$, then $\mathbf{d}^{(i+1)} = \mathbf{d}^{(i)}/3$ if $r < 0.5$.

4 Demonstration Case Studies and Benchmarking

This section summarizes numerical verification of the optimization procedure introduced in Section 3. It is based on two microstrip components, and includes evaluation of the reliability and computational efficiency of the optimization process, as well as comparisons with several benchmark methods characterized in Section 4.2.

4.1 Verification Circuits

Verification experiments are based on the circuits shown in Fig. 4. These are a dual-band power divider operating at 2.4 GHz and 3.8 GHz (Circuit I) [33], and a compact branch-line coupler (BLC) operating at 1.5 GHz (Circuit II) [34]. The relevant circuit details have been gathered in Table 1. The EM simulation models of both circuits are implemented in CST Microwave Studio and evaluated using the time-domain solver.

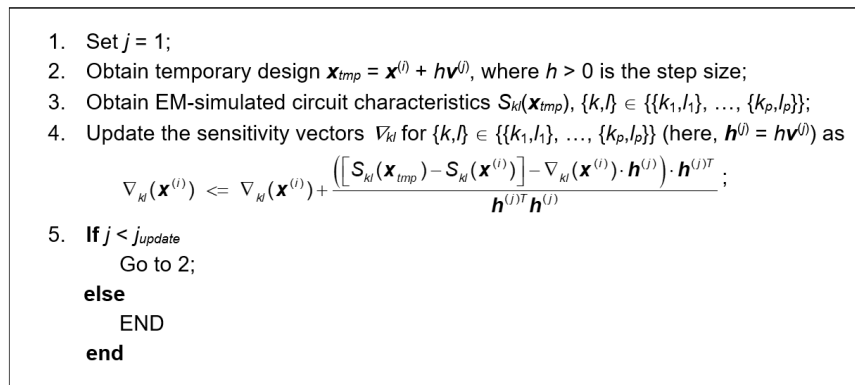


Fig. 2. Sparse sensitivity updates using principal directions. The step size h is set to a fraction of mm (between 0.02 to 0.1), a typical value for FD carried out on EM-simulated responses.

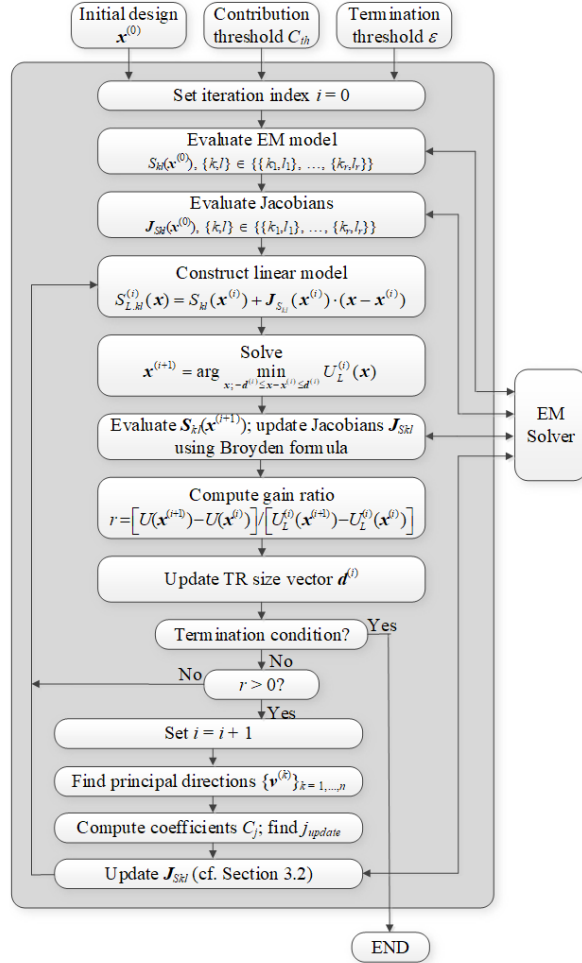


Fig. 3. Flow diagram of the proposed accelerated optimization algorithm with sparse sensitivity updates using principal directions.

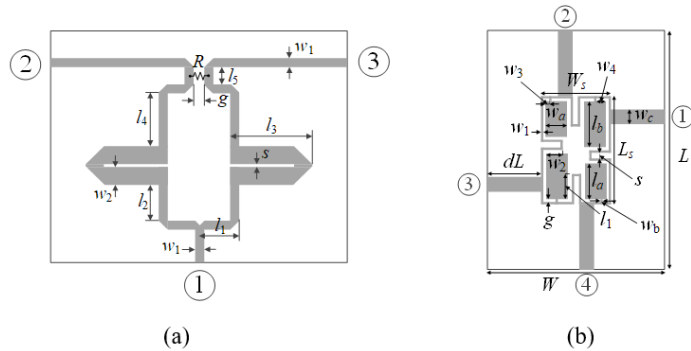


Fig. 4. Verification circuits: (a) dual-band power divider (Circuit I) [33], (b) miniaturized branch-line coupler (Circuit II) [34].

Table 2. Verification circuits

	Case study	
	Circuit I	Circuit II
Substrate	AD250 ($\epsilon_r = 2.5$, $h = 0.81$ mm, $\tan\delta = 0.0018$)	RO4003 ($\epsilon_r = 3.5$, $h = 0.76$ mm, $\tan\delta = 0.0027$)
Design parameters	$\mathbf{x} = [l_1 \ l_2 \ l_3 \ l_4 \ l_5 \ s \ w_2]^T$	$\mathbf{x} = [g \ l_1r \ l_a \ l_b \ w_1 \ w_{2r} \ w_{3r} \ w_{4r} \ w_a \ w_b]^T$
Other parameters	$w_1 = 2.2$, $g = 1$ mm	$L = 2dL + L_s$, $L_s = 4w_1 + 4g + s + l_a + l_b$, $W = 2dL + W_s$, $W_s = 4w_1 + 4g + s + 2w_a$, $l_1 = l_b l_{1r}$, $w_2 = w_a w_{2r}$, $w_3 = w_{3r} w_a$, and $w_4 = w_{4r} w_a$.
Design specifications	<ul style="list-style-type: none"> • Operating frequencies: $f_1 = 2.4$ GHz and $f_2 = 3.8$ GHz • Goal 1: minimize input matching S_{11}, and output matching S_{22}, S_{33}, at both f_1 and f_2 • Goal 2: minimize isolation S_{23} at both f_1 and f_2 • Goal 3: ensure equal power split (note: this is implied by the structure symmetry) 	<ul style="list-style-type: none"> • Operating frequency $f_0 = 1.5$ GHz • Goal 1: minimize matching S_{11} and isolation S_{41} at f_0 • Goal 2: ensure equal power split, i.e., $S_{21} = S_{31}$ at f_0

4.2 Experimental Setup

The algorithm of Section 3 has been compared to four benchmark routines briefly characterized in Table 2. Each procedure has been executed ten times starting from a random initial design. The results statistics discussed in Section 4.3 account for the average performance of the search process.

4.3 Results and Discussion

Tables 3 and 4 provide the results obtained for Circuits I and II, respectively. The circuit frequency characteristics at the initial and optimized designs obtained for the selected runs of our algorithm can be found in Figs. 6 and 7. As mentioned earlier, the results are in the form of statistics based on ten independent runs of the proposed and benchmark algorithms.

The performance of the presented algorithm in comparison to the benchmark can be characterized as follows:

- The algorithm of Section 3 performs consistently for both circuits in terms of all considered factors (computational complexity, reliability, and solution repeatability). The quality of optimized designs is comparable to Algorithm I (the reference);
- The achieved CPU savings are as high as forty percent for Circuit I and over fifty percent for Circuit II. These figures are higher for Algorithms II through IV (which are all accelerated procedures). The quality of the optimized designs is better than for the benchmark procedures.

Another important advantage of the proposed technique is the simplicity of its setup. Apart from the termination threshold, there is only one control parameter C_{th} , the meaning of which is intuitive as explained in Section 3.2.

Table 2. Benchmark algorithms

Algorithm	Operating principles
I	<ul style="list-style-type: none"> Conventional TR algorithm with numerical derivatives, cf. Section 2.2 This method is used as a reference to compute computational savings that can be obtained w.r.t. full finite-differentiation-based sensitivity estimation
II	<ul style="list-style-type: none"> Accelerated version of the reference TR procedure (details in [29]) Sensitivity updates omitted for the parameters for which relative design relocation is small (with respect to the trust-region size in the current iteration), i.e., $\phi_k^i = \left x_k^{(i+1)} - x_k^{(i)} \right / d_k^{(i)}, k = 1, \dots, n,$ where $x_k^{(i)}$ and $x_k^{(i+1)}$ are the kth entries of the parameter vectors $\mathbf{x}^{(i)}$ and $\mathbf{x}^{(i+1)}$ from the last two iterations, respectively; $d_k^{(i)}$ refers to the kth element of the TR size vector $\mathbf{d}^{(i)}$ FD is omitted for the parameters, for which ϕ_k^i factors are below a user-defined threshold For each gradient vector, FD update is enforced at least once every few iterations Control parameter N_{iter}: the maximum admissible number of iterations without FD (typically from 3 to 5; in this work we set $N_{iter} = 3$); increasing N_{iter} likely leads to cost savings but may be detrimental for the design quality
III	<ul style="list-style-type: none"> Accelerated version of the reference TR procedure (details in [30]) Sensitivity updates realized with a Broyden formula (BF) for parameters that are sufficiently aligned with the direction of the recent design relocation. The alignment is quantified as $\gamma_k^{(i)} = \left \mathbf{h}^{(i)T} \mathbf{e}^{(k)} \right / \left\ \mathbf{h}^{(i)} \right\ , \quad k = 1, \dots, n$ where $\mathbf{e}^{(k)} = [0 \dots 0 \ 1 \ 0 \dots 0]^T$ with one on the kth position, is the kth standard basis vector, and $\mathbf{h}^{(i+1)} = \mathbf{x}^{(i+1)} - \mathbf{x}^{(i)}$. The kth gradient vector is updated using BF if $\gamma_k^{(i)}$ is larger than a user-defined threshold γ_{min} Control parameter $0 \leq \gamma_{min} \leq 1$ allows for adjusting the trade-offs between the CPU cost and design quality. Higher γ_{min} makes the condition for using BF more rigorous, and a larger number of gradient vectors is updated using finite differentiation leading to improved quality but lower savings In this work, $\gamma_{min} = 0.9$, as recommended in [30]
IV	<ul style="list-style-type: none"> Accelerated version of the reference TR algorithm (details in [35]) Sensitivity updates based on detected stable sensitivity patterns across the algorithm iterations. Let $\nabla_S = [\nabla_1 \dots \nabla_n]^T$ be the gradient vector of relevant system responses, where ∇_k stands for sensitivity w.r.t the k-th parameter, $k = 1, \dots, n$. Also, let $\nabla_k^{(i)}(f)$ and $\nabla_k^{(i-1)}(f)$ refer to the k-th component of the gradient ∇_S in the ith and $(i-1)$th iteration. The gradient change factors are defined as $d_k^{(i+1)} = \underset{f \in \mathcal{F}}{mean} \left(2 \cdot \frac{\left \nabla_k^{(i)}(f) \right - \left \nabla_k^{(i-1)}(f) \right }{\left \nabla_k^{(i)}(f) \right + \left \nabla_k^{(i-1)}(f) \right } \right)$ i.e., represent relative gradient changes averaged over the frequency range of interest. Let $d_{min}^{(i)} = \min\{k = 1, \dots, n : d_k^{(i)}\}$ and $d_{max}^{(i)} = \max\{k = 1, \dots, n : d_k^{(i)}\}$. Using these, the numbers $N_k^{(i)}$ of future iterations without FD-based updates for the k-th parameter are set to $N_k^{(i)} = \left\lceil N_{max} + a^{(i)} (d_k^{(i)} - d_{min}^{(i)}) \right\rceil$ where $a^{(i)} = (N_{max} - N_{min}) / (d_{min}^{(i)} - d_{max}^{(i)})$ ($\lceil \cdot \rceil$ is the nearest integer function). N_{min}/N_{max} are the minimum/maximum number of iterations without FD (control parameters). Remark: sensitivity update using FD is executed at least once per N_{max} iterations, and not more often than every N_{min} iterations. Here, we use $N_{max} = 5$ and $N_{min} = 1$ (cf. [35])

Table 3. Optimization results for Circuit I

Algorithm	Performance figure				
	CPU Cost ¹	Cost savings ²	$\max S_{11} $ ³	$\Delta \max S_{11} $ ⁴	Std $\max S_{11} $ ⁵
Algorithm I	99.8	–	–31.6 dB	–	4.5 dB
Algorithm II	77.5	22.4 %	–28.6 dB	3.0 dB	6.0 dB
Algorithm III	81.9	17.9 %	–28.1 dB	3.5 dB	5.8 dB
Algorithm IV	67.9	32.1 %	–29.5 dB	2.1 dB	5.7 dB
This work ($C_{th} = 0.8$) ⁶	59.8	40.1 %	–30.3 dB	1.3 dB	4.3 dB
This work ($C_{th} = 0.9$) ⁶	60.8	39.1 %	–30.6 dB	1.0 dB	4.2 dB

¹Number of equivalent EM evaluation of the circuit (averaged over ten algorithm runs).

²Relative savings in percent w.r.t. Algorithm I.

³Objective function value, averaged over ten algorithm runs.

⁴Degradation of the objective function value w.r.t. the TR algorithm in dB, averaged over ten algorithm runs.

⁵Standard deviation of the objective function value in dB across the set of ten algorithm runs.

⁶Index j_{update} selected as in (14).

Table 4. Optimization results for Circuit II

Algorithm	Performance figure				
	CPU Cost ¹	Cost savings ²	$\max S_{11} $ ³	$\Delta \max S_{11} $ ⁴	Std $\max S_{11} $ ⁵
Algorithm I	84.6	–	–20.9 dB	–	1.5 dB
Algorithm II	67.4	20.0 %	–20.7 dB	0.2 dB	2.1 dB
Algorithm III	43.6	48.4 %	–18.8 dB	2.1 dB	3.8 dB
Algorithm IV	64.2	24.1 %	–20.7 dB	0.2 dB	1.8 dB
This work ($C_{th} = 0.8$) ⁶	38.3	54.7 %	–21.9 dB	–1.0 dB	2.9 dB
This work ($C_{th} = 0.9$) ⁶	51.5	39.1 %	–21.5 dB	–0.6 dB	3.4 dB

¹⁻⁵As in Table 4.

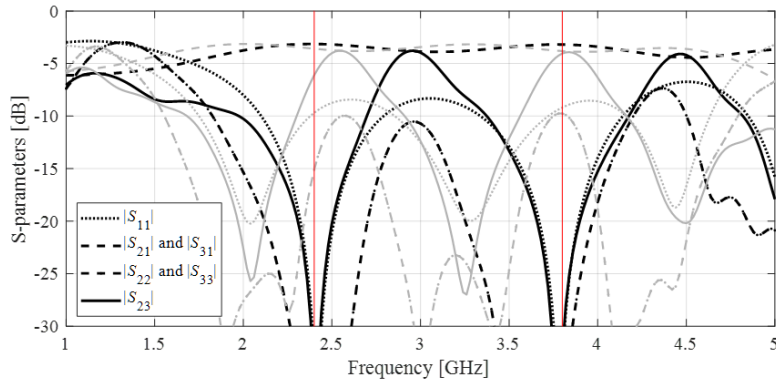


Fig. 6. S-parameters of Circuit I for the selected run of the proposed algorithm. Initial and optimized designs are shown using grey and black lines, respectively. The vertical lines mark the target operating frequencies.

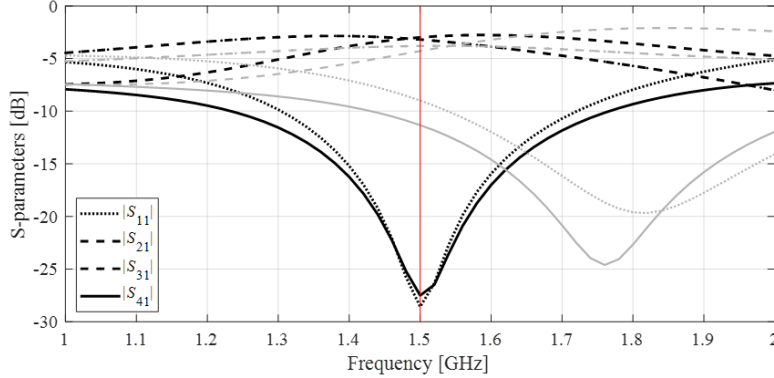


Fig. 6. S-parameters of Circuit II for the selected run of the proposed algorithm. Initial and optimized designs are shown using grey and black lines, respectively. The vertical line marks the target operating frequency.

Also, as shown in Tables 3 and 4, the algorithm performance is only weakly dependent on the value C_{th} . On the other hand, the operation of the benchmark techniques depends on a larger number of control parameters, the setup of which is more intricate (cf. [29], [30], [35]).

The improvements achieved by the presented method over the benchmark is mainly related to the fact that the sensitivity updates are not restricted to the coordinate system axes, which was the case for the earlier algorithms.

5 Conclusions

This paper proposed a novel technique for accelerated local parameter tuning of microwave components. Our methodology capitalizes on restricting the finite-differentiation-based sensitivity updates to a selected set of principal directions established as having the major influence on the system response variability. Extensive numerical experiments indicate superiority of the proposed technique over several benchmark methods, including previously reported expedited optimization frameworks. The future work will be focused on achieving further acceleration through the incorporation of variable-resolution simulation models.

Acknowledgement

The authors would like to thank Dassault Systemes, France, for making CST Microwave Studio available. This work is partially supported by the Icelandic Centre for Research (RANNIS) Grant 206606 and by National Science Centre of Poland Grant 2020/37/B/ST7/01448.

References

1. Gumber, K., Dejous, C., Hemour, S.: Harmonic reflection amplifier for widespread backscatter internet-of-things. *IEEE Trans. Microwave Theory Techn.*, **69**(1), pp. 774–785 (2021)
2. Gugliandolo, G., Naishadham, K., Neri, G., Fernicola, V. C., Donato, N.: A novel sensor-integrated aperture coupled microwave patch resonator for humidity detection. *IEEE Trans. Instrumentation Meas.*, **70**, pp. 1–11, Art no. 9506611 (2021)
3. Pradhan, N. C., Subramanian, K. S., Barik, R. K., Cheng, Q. S.: Design of compact substrate integrated waveguide based triple- and quad-band power dividers. *IEEE Microwave Wireless Comp. Lett.*, **31**(4), pp. 365–368 (2021)
4. Li, Q., Yang, T.: Compact UWB half-mode SIW bandpass filter with fully reconfigurable single and dual notched bands. *IEEE Trans. Microwave Theory Techn.*, **69**(1), pp. 65–74 (2021)
5. Liu, H., Fang, S., Wang, Z., Fu, S.: Design of arbitrary-phase-difference transdirectional coupler and its application to a flexible Butler matrix. *IEEE Trans. Microwave Theory Techn.*, **67**(10), pp. 4175–4185 (2019)
6. Sieganschin, A., Tegowski, B., Jaschke, T., Jacob, A. F.: Compact diplexers with folded circular SIW cavity filters. *IEEE Trans. Microwave Theory Techn.*, **69**(1), pp. 111–118 (2021)
7. Zhu, Y., Dong, Y.: A novel compact wide-stopband filter with hybrid structure by combining SIW and microstrip technologies. *IEEE Microwave Wireless Comp. Lett.*, **31**(7), pp. 841–844 (2021)
8. Rayas-Sanchez, J.E., Koziel, S., Bandler, J.W.: Advanced RF and microwave design optimization: a journey and a vision of future trends. *IEEE J. Microwaves*, **1**(1), pp. 481–493, (2021)
9. Bayraktar, Z., Komurcu, M., Bossard, J. A., Werner, D. H.: The wind driven optimization technique and its application in electromagnetics. *IEEE Trans. Ant. Propag.*, **61**(5), pp. 2745–2757 (2013)
10. Pietrenko-Dabrowska, A., Koziel, S., Al-Hasan, M.: Expedited yield optimization of narrow- and multi-band antennas using performance-driven surrogates. *IEEE Access*, **9**, pp. 143104–143113 (2020)
11. Koziel, S., Mosler, F., Reitzinger, S., Thoma, P.: Robust microwave design optimization using adjoint sensitivity and trust regions. *Int. J. RF Microwave CAE*, **22**(1), pp. 10–19 (2012)
12. Feng, F., Zhang, J., Zhang, W., Zhao, Z., Jin, J., Zhang, Q.: Coarse- and fine-mesh space mapping for EM optimization incorporating mesh deformation. *IEEE Microwave Wireless Comp. Lett.*, **29**(8), pp. 510–512 (2019)
13. Koziel, S.: Fast simulation-driven antenna design using response-feature surrogates. *Int. J. RF & Microwave CAE*, **25**(5), pp. 394–402 (2015)
14. Jin, J., Feng, F., Na, W., Zhang, J., Zhang, W., Zhao, Z., Zhang, Q.J.: Advanced cognition-driven EM optimization incorporating transfer function-based feature surrogate for microwave filters. *IEEE Trans. Microwave Theory Techn.*, **69**(1), pp. 15–28 (2021)
15. Koziel, S., Leifsson, L.: *Simulation-driven design by knowledge-based response correction techniques*. Springer, New York (2016)
16. Van Nechel, E., Ferranti, F., Rolain, Y., Lataire, J.: Model-driven design of microwave filters based on scalable circuit models. *IEEE Trans. Microwave Theory Techn.*, **66**(10), pp. 4390–4396 (2018)
17. Li, Y., Xiao, S., Rotaru, M., Sykulski, J. K.: A dual kriging approach with improved points selection algorithm for memory efficient surrogate optimization in electromagnetics. *IEEE Trans. Magn.*, **52**(3), pp. 1–4, Art no. 7000504 (2016)

18. Barmuta, P., Ferranti, F., Gibiino, G.P., Lewandowski, A., Schreurs, D.M.M.P.: Compact behavioral models of nonlinear active devices using response surface methodology. *IEEE Trans. Microwave Theory and Tech.*, **63**(1), pp. 56–64 (2015)
19. Brihuega, A., Anttila, L., Valkama, M.: Neural-network-based digital predistortion for active antenna arrays under load modulation. *IEEE Microwave Wireless Comp. Lett.*, **30**(8), pp. 843–846 (2020)
20. Liu, B., Yang, H., and Lancaster, M. J.: Global optimization of microwave filters based on a surrogate model-assisted evolutionary algorithm. *IEEE Trans. Microwave Theory Techn.*, **65**(6), pp. 1976–1985 (2017)
21. Toktas, A., Ustun, D., Tekbas, M.: Multi-objective design of multi-layer radar absorber using surrogate-based optimization. *IEEE Trans. Microwave Theory Techn.*, **67**(8), pp. 3318–3329 (2019)
22. Zhang, J., Zhang, C., Feng, F., Zhang, W., Ma, J., Zhang, Q.J.: Polynomial chaos-based approach to yield-driven EM optimization. *IEEE Trans. Microwave Theory Techn.*, **66**(7), pp. 3186–3199 (2018)
23. Zhang, J., Feng, F., Jin, J., Zhang, Q.-J.: Efficient yield estimation of microwave structures using mesh deformation-incorporated space mapping surrogates. *IEEE Microwave Wireless Comp. Lett.*, **30**(10), pp. 937–940 (2020)
24. Koziel, S., Unnsteinsson, S.D.: Expedited design closure of antennas by means of trust-region-based adaptive response scaling. *IEEE Ant. Wireless Prop. Lett.*, **17**(6), pp. 1099–1103 (2018)
25. Li, S., Fan, X., Laforge, P. D., Cheng, Q. S.: Surrogate model-based space mapping in postfabrication bandpass filters’ tuning. *IEEE Trans. Microwave Theory Techn.*, **68**(6), pp. 2172–2182 (2020)
26. Lim, D. K., Woo, D. K., Yeo, H. K., Jung, S. Y., Ro, J. S., Jung, H. K.: A novel surrogate-assisted multi-objective optimization algorithm for an electromagnetic machine design. *IEEE Trans. Magn.*, **51**(3), paper 8200804 (2015)
27. An, S., Yang, S., Mohammed, O. A.: A Kriging-assisted light beam search method for multi-objective electromagnetic inverse problems. *IEEE Trans. Magn.*, **54**(3), paper 7001104 (2018)
28. Koziel, S.: Improved trust-region gradient-search algorithm for accelerated optimization of wideband antenna input characteristics. *Int. J. RF & Microwave CAE*, **29**(4), e21567 (2019)
29. Pietrenko-Dabrowska, A., Koziel, S.: Computationally-efficient design optimization of antennas by accelerated gradient search with sensitivity and design change monitoring. *IET Microwaves Ant. Prop.*, **14**(2), pp. 165–170 (2020)
30. Pietrenko-Dabrowska, A., Koziel, S.: Numerically efficient algorithm for compact microwave device optimization with flexible sensitivity updating scheme. *Int. J. RF & Microwave CAE*, **29**(7) (2019)
31. Conn, A.R., Gould, N.I.M., Toint, P.L., *Trust Region Methods*, MPS-SIAM Series on Optimization (2000)
32. Broyden, C.G.: A class of methods for solving nonlinear simultaneous equations. *Math. Comp.*, **19**, pp. 577–593 (1965)
33. Lin, Z., Chu, Q.-X.: A novel approach to the design of dual-band power divider with variable power dividing ratio based on coupled-lines. *Prog. Electromagn. Res.*, **103**, pp. 271–284 (2010)
34. Tseng, C., Chang, C.: A rigorous design methodology for compact planar branch-line and rat-race couplers with asymmetrical T-structures. *IEEE Trans. Microwave Theory Techn.*, **60**(7), pp. 2085–2092 (2012)
35. Pietrenko-Dabrowska, A., Koziel, S.: Expedited antenna optimization with numerical derivatives and gradient change tracking. *Eng. Comp.*, **37**(4), pp. 1179–1193 (2019)